

RESEARCH OF THE TECHNOLOGICAL PROCESS OF GRANULATION OF BULK AGRICULTURAL MATERIALS

ДОСЛІДЖЕННЯ ТЕХНОЛОГІЧНОГО ПРОЦЕСУ ГРАНУЛЮВАННЯ СИПКИХ СІЛЬСЬКОГОСПОДАРСЬКИХ МАТЕРІАЛІВ

Volodymyr BULGAKOV¹⁾, Adolfs RUCINS*²⁾, Yevhen IHNATIEV^{3,4)}, Serhiy STEPANENKO⁵⁾, Lucretia POPA⁶⁾, Simone PASCUZZI⁷⁾, Ivan HOLOVACH¹⁾, Oleksandra TROKHANIAK¹⁾

¹⁾National University of Life and Environmental Sciences of Ukraine / Ukraine;

²⁾Latvia University of Life Sciences and Technologies / Latvia;

³⁾Estonian University of Life Sciences / Estonia;

⁴⁾Dmytro Motorny Tavria State Agrotechnological University / Ukraine;

⁵⁾Institute of Mechanics and Automation of Agricultural Production of the National Academy of Agrarian Sciences of Ukraine;

⁶⁾National Institute of Research–Development for Machines and Installations Designed for Agriculture and Food Industry–INMA, Bucharest / Romania;

⁷⁾University of Bari Aldo Moro / Italy

*Corresponding author's E-mail: adolfs.rucins@lbtu.lv; vbulgakov@meta.ua

DOI: <https://doi.org/10.35633/inmateh-75-63>

Keywords: density, die, deformation, compaction, friction, resistance, granulation process, bulk materials

ABSTRACT

This research addresses the axisymmetric problem in the theory of granulation of porous bodies, with practical application in calculating the forces involved in the granulation of dispersed bulk materials such as chips, granules, and other agricultural and woodworking waste. For such materials, the shape of the particles (structural elements) is generally irregular and not geometrically well-defined. This characteristic served as the basis for adopting a continuum model of porous media. In this model, the material is treated as a continuous substance that fills all available layers of bulk space, allowing for the mechanical behavior of materials with internal pores or voids to be accurately described. The pores within the material are considerably smaller compared to other characteristic dimensions of the material's properties. In the continuum model, the mechanical characteristics of the material, such as stress, strain, and compaction, are described by mathematical equations that account for the material's physical properties and its behavior under loading. By reducing this model to a two-dimensional spatial form, a closed-form analytical solution was obtained using a general method for solving the differential equations of equilibrium along with the Huber–Mises energy condition for plasticity. The following assumptions were adopted as working hypotheses: radial and tangential stresses are equal, and the lateral pressure coefficient is equal to the proportional granulation density. Given that the problem is solved in a general form, the solution should be regarded as methodological, that is, it can be applied to any loading scheme exhibiting axial symmetry. Transcendental equations were derived to describe the deformation compaction process of a porous body. These equations account for both the ideal granulation process and the influence of contact friction forces. As a result of developing a solution method for these equations, dependencies were obtained for calculating the local characteristics of the stress state during granulation, as well as for integral parameters of the process, such as compaction and deformation work.

АНОТАЦІЯ

Дане дослідження присвячене вирішенню вісе-симетричної задачі теорії гранулювання пористих тіл з практичним застосуванням у вигляді силового розрахунку процесів гранулювання дисперсних сипучих матеріалів: стружкових, гранульованих та інших відходів сільськогосподарського виробництва і деревообробки. Для таких матеріалів форма частинок (структурних елементів) не є геометрично правильною або взагалі визначеною. Це служило підґрунтям для того, що в основу вирішення була покладена континуальна модель пористого тіла, яка дозволяє описувати механічну поведінку матеріалів, які мають пори або порожнини в своїй структурі. В даній моделі матеріал розглядається як неперервна речовина, що заповнює усі доступні шари сипкого простору. Пори у матеріалі вважаються невеликими в порівнянні зі значеннями інших властивостей матеріалу.

У континуальній моделі, механічні характеристики матеріалу, такі як напруження, деформація та тиск, описуються математичними рівняннями, що враховують фізичні властивості матеріалу та його поведінку під навантаженням. Ця модель застосовується для аналізу різних видів механічних деформацій та взаємодії матеріалів, включаючи стискання, розтягування, згин, обертання тощо. В результаті зведення даної моделі до двовимірної просторової моделі отримано замкнене аналітичне рішення методом спільного вирішення диференціальних рівнянь рівноваги та енергетичної умови пластичності Губера-Мізеса. В якості робочих гіпотез прийняті наступні припущення: радіальне і тангенціальне напруження рівні, коефіцієнт бічного тиску рівний пропорційній щільності гранулювання. З огляду на те, що задача вирішена у загальному вигляді, саме рішення слід розглядати як методологічне, тобто може бути використано для будь-якої схеми навантаження, яка виявляє осьову симетрію. Були отримані трансцендентні рівняння, які описують процес деформаційного ущільнення пористого тіла. Ці рівняння враховують як ідеальний процес гранулювання, так і вплив сил контактного тертя. Внаслідок розробки методу розв'язання цих рівнянь були отримані залежності для обчислення локальних характеристик напруженого стану в процесі гранулювання, а також для інтегральних параметрів цього.

INTRODUCTION

Porous bodies include materials that can be granular or other bulk substances (Pisarenko & Mozharovsky, 1981; Bertram, 2012; Hashiguchi & Yamakawa, 2012; Haupt, 2002; Lubliner, 1990; Zhou et al., 2021; Aruffo et al., 2024; Zheng et al., 2017; Uniyal et al., 2020). Zhou et al., (2021), present the shear strength behavior of glass beads with two particular sizes under the influence of 0-5% liquid and hydrated lime (HL) contents. Experimental work was performed to analyze the influence of liquid-powder mixture ratios on a wet granular system under various loading stresses. Hence, evaluating bulk density and shear resistance is crucial for assessing the growth and strength of agglomerated products (Aruffo et al., 2024; Zheng et al., 2017; Unival et al., 2020).

In the classification according to the physical and mechanical properties of particles (structural elements), these materials belong to the category of structurally heterogeneous (Landau, & Lifshits, 2013; Gurson, 1977; Bettinotti et al., 2017; Aruffo et al., 2022). Usually, the shape of the particles does not have a geometrically correct structure or may even be undefined, which casts doubt on the possibility of using the contact-discrete model of deformation compaction for such materials. In such situations it is more appropriate to use a model that treats the material as a compressible continuum and takes into account rheological characteristics, such as the yield strength (Lu & Li, 2017; Bratishko, 2020; Bratishko, 2014; Boltyanska, 2018; Salman et al., 2007; Probst & Ileleji, 2016).

Probst & Ileleji, (2016), presented a laboratory-scale batch drum granulation process used to produce granules from dried distillers grains with solubles (DDGS). This was achieved by adding condensed distillers solubles (CDS) as a binder to wet distillers grains (WDG), both of which are coproducts of the corn dry-grind ethanol process, under varying formulation and process conditions. A full factorial experimental design was employed to test all combinations of factor levels, including the amount of CDS binder, CDS solids content, screen size opening, and residence time. These characteristics allow for the assessment of the material's resistance to deformation.

Even though several studies have described the impact of granulation process parameters on granule size distribution, granules density, and flowability (Benali et al., 2009; Liu et al., 2013; Mangwandi et al., 2013), no systematic investigation has yet reported how these variables influence the granule hardness and compression properties of granules. Granule hardness could be one of the important properties in tablet formulation because granules having insufficient hardness are extremely fragile leading to compromise on quality. On the other hand, if the granules are extremely hard, this may compromise the compressibility. Meanwhile, compression behavior of granules might be altered by process variables. However, detailed studies are very limited on how process variables influence the compression behavior of granules. Heckle plot analysis can be commonly used for the analysis of compression behavior of pharmaceutical excipients. Therefore, one of the objectives of the present study was to investigate the impact of process variables on granule hardness and compression behavior of granules.

MATERIALS AND METHODS

The solution of the axisymmetric problem in the granulation theory of porous bodies involves determining the local characteristics of the stress state during granulation as a function of spatial coordinates, as well as key integral parameters such as compression, force, and deformation work (Pisarenko & Mozharovsky, 1981; Bertram, 2012; Hashiguchi & Yamakawa, 2012; Haupt, 2002; Lubliner, 1990). For modeling purposes, the porous body is represented as a solid, compressible, rigid-plastic material with a defined yield point. The granulation process of the porous material is carried out within a die, as illustrated in Fig. 1.

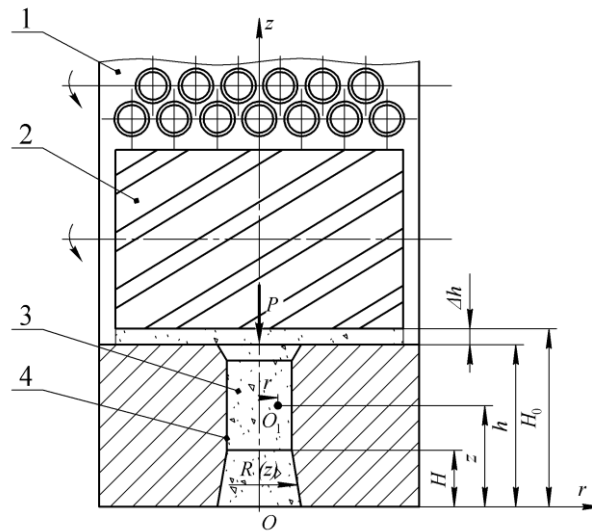


Fig. 1 – Technological scheme of granulation of a porous body in a die spinneret

1 – die; 2 – roller; 3 – porous material; 4 – spinneret

During the granulation process, the side surface of the die is modeled as a body of revolution. At any given moment under axisymmetric loading, it can be described by the equation $R=R(z)$. In the first stage of analysis, force calculations are performed without accounting for contact friction forces.

The following notations are used in this research: H_0, H – initial and final granulation height; h – current granule formation height; Δh – deformation path (compaction); R – radius of granule formation at a given section z ; ρ_0 – current material density; ρ_m – maximum material density (granules); $\mu = \rho_0/\rho_m$ – relative granule density; μ_0, μ_k – initial and final values of relative density; $\varepsilon = 1-\mu$ – relative porosity; σ_m – yield strength of the material; η – plasticity constant; f – coefficient of friction.

For any point in the deformation process the differential equations of equilibrium in cylindrical coordinates are written as follows (Pisarenko & Mozharovsky, 1981; Hashiguchi & Yamakawa, 2012; Landau & Lifshits, 2013; Bettinotti et al., 2017; Lu & Li, 2017):

$$\frac{\partial \sigma_R}{\partial R} + \frac{\partial \tau_{Rz}}{\partial z} + \frac{\sigma_R - \sigma_\varphi}{R} = 0 \tag{1}$$

$$\frac{\partial \tau_{zR}}{\partial R} + \frac{\partial \sigma_z}{\partial z} + \frac{\tau_{zR}}{R} = 0 \tag{2}$$

The plasticity condition is applied in the following form (Landau & Lifshits, 2013; Bratishko, 2020):

$$(\sigma_R - \sigma_\varphi)^2 + (\sigma_\varphi - \sigma_z)^2 + (\sigma_z - \sigma_R)^2 + 6 \cdot \tau_{Rz}^2 = 2 \cdot \sigma_m^2 \tag{3}$$

An elementary volume of a granule with the corresponding stress tensor components is shown in Fig. 2. Under axisymmetric loading conditions in meridional planes passing through the z -axis, the tangential stresses are zero, and the stress components are independent of the coordinate φ .

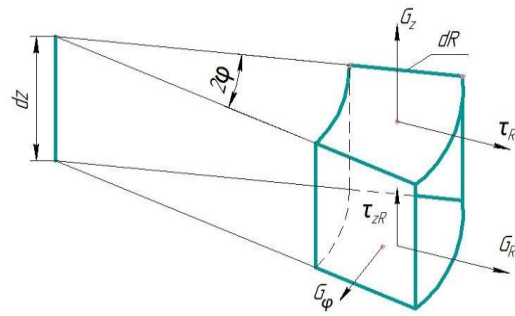


Fig. 2 – Schematic diagram of the elementary volume of the deformation element together with the components of the stress tensor during the granulation process

According to the Haar-Karman condition of full plasticity (Pisarenko & Mozharovsky, 1981; Salman et al., 2007; Payne et al., 2016), when the movement of the material in the radial direction is limited by the die wall, and tangential movement is kinematically prohibited due to the symmetrical separation of the surface in the planes φ, it can be assumed that $\sigma_\phi = \sigma_R$. In addition, the normal radial stress σ_R is directly proportional to the density of the material during the granulation process and within the limits $\mu = 1$ reaching value σ_z (Bratishko, 2014; Boltianska, 2018; Pietsch, 2002):

$$\sigma_\phi = \sigma_R = \mu \cdot \sigma_z \tag{4}$$

Under conditions of fully-sided non-uniform compression, where the spherical component of the stress tensor significantly dominates the deviatoric component, a relationship is established between the normal axial (or radial) stress and the deviatoric stress. The relationship between the tangential and normal radial stresses is linear. In practice, the relative density of granules during the granulation process μ is approximately equal to the lateral pressure coefficient.

Relative density, as well as the deformation path or time, are common variables of the granulation process. However, for the studied fixed moment it is considered a constant when calculating the stress state.

Taking into account the proposed assumption (4), the law of paired tangential stresses $\tau_{Rz} = \tau_{zR} = \tau$ and the corresponding designation, $\sigma = \sigma_z$ the system of equations (1) – (3) can be expressed as follows:

$$\mu \frac{\partial \sigma}{\partial R} + \frac{\partial \tau}{\partial z} = 0 \tag{5}$$

$$\frac{\partial \tau}{\partial R} + \frac{\partial \sigma}{\partial z} + \frac{\tau}{R} = 0 \tag{6}$$

$$(1 - \mu)^2 \cdot \sigma^2 + 3 \cdot \tau^2 = \sigma_m^2 \tag{7}$$

The plasticity condition (Aruffo et al., 2024) establishes the following relationship between the components of the stress tensor:

$$\sigma = \varepsilon^{-1} \cdot (\sigma_m^2 - 3 \cdot \tau^2)^{0.5} \tag{8}$$

$$\tau = 0.58 \cdot (\sigma_m^2 - \varepsilon^2 \cdot \sigma^2)^{0.5} \tag{9}$$

For the following calculations we will create a table of derivatives of these expressions, using the concept, known in mathematics, of taking the derivative of an implicitly defined function and, taking into account (Lublinter, 1990), we will obtain:

For the subsequent calculations, a table of derivatives of these expressions will be will constructed using the mathematical concept of taking the derivative of an implicitly defined function. Taking into account the approach described in Lubliner (1990), it is obtained:

$$\dot{\sigma}_R = 3 \cdot \varepsilon^{-1} \cdot \tau \cdot \dot{\tau}_R \cdot (\sigma_m^2 - 3 \cdot \tau^2)^{-0.5} = -3 \cdot \tau \cdot \dot{\tau}_R \cdot \varepsilon^{-2} \cdot \sigma^{-1} = -\dot{\tau}_z \cdot \mu^{-1} \tag{10}$$

$$\dot{\sigma}_z = 3 \cdot \varepsilon^{-1} \cdot \tau \cdot \dot{\tau}_z \cdot (\sigma_m^2 - 3 \cdot \tau^2)^{-0.5} = -3 \cdot \tau \cdot \dot{\tau}_z \cdot \varepsilon^{-2} \cdot \sigma^{-1} \tag{11}$$

$$\dot{\tau}_R = -0.58 \cdot \varepsilon^2 \cdot \sigma \cdot \dot{\sigma}_R \cdot (\sigma_m^2 - \varepsilon^2 \cdot \sigma^2)^{-0.5} \tag{12}$$

$$\dot{\tau}_z = -0.58 \cdot \varepsilon^2 \cdot \sigma \cdot \dot{\sigma}_z \cdot (\sigma_m^2 - \varepsilon^2 \cdot \sigma^2)^{-0.5} = -\mu \cdot \dot{\sigma}_R \tag{13}$$

In the above dependencies (10)-(13) $\sigma(z, R); \tau(z, R)$ represent the required stresses (functions of independent coordinates z, R) at a given relative density μ of granules in the granulation process.

RESULTS

For the granulation process, the geometric interpretation of the plasticity condition is as follows: The plasticity condition (7) can be geometrically represented as a circle with radius σ_m , where each point corresponds to a stress state that induces and sustains plastic deformation of the material. In Fig. 3, the axes σ and z are depicted at a 90° angle, resembling a conventional plane of a nominal section.

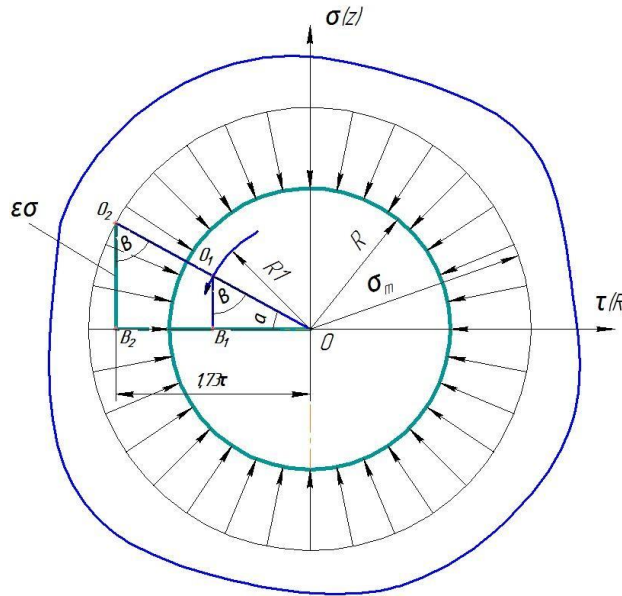


Fig. 3 – Geometric interpretation of the plasticity condition in the process of granulation of bulk materials

For each point of the elementary volume of deformation (suppose that this is a point O_1 with coordinates z, R_1) there corresponds the desired stress tensor $\sigma \tau$ (point O_2 on the plasticity circle) with projections on the stress axes (1.73τ) and ($\varepsilon \sigma$). The angles of the right triangle OO_2B_2 are determined by the following relationships:

$$\alpha = \sin^{-1} [\varepsilon \cdot \sigma \cdot \sigma_m^{-1}] \tag{14}$$

$$\beta = \sin^{-1} [1.73 \cdot \tau \cdot \sigma_m^{-1}] = \tan^{-1} [1.73 \cdot \tau \cdot \varepsilon^{-1} \cdot \sigma^{-1}] \tag{15}$$

$$\alpha + \beta = \pi / 2 \tag{16}$$

When considering the axis of symmetry z , there is no tangential stress $\tau (R_1=0; \tau=0)$ throughout the entire height of the die during the granulation process, regardless of the degree of compression deformation. At the same time the normal stress σ , according to the plasticity condition (7), reaches its maximum value: $\sigma = \varepsilon^{-1} \sigma_m$.

However, it should be noted that by increasing the distance from axis z in the radial direction $0 \leq R_1 \leq R$; σ – decreases, while τ increases. These indicators reach extreme values at $R_1=R$. The angle α of triangle OO_2B_2 varies from 90° to 0° , and the angle β varies from 0° to 90° . The sum of these two angles is 90° , which, similar to equation (7), expresses the mathematical definition of the plasticity condition. On the side surface of the die during the granulation process, there is stress in the radial direction at $R_1=R$, but no deformation occurs. When relative density increases $\mu_0 \leq \mu \leq 1$, $\sigma \rightarrow \infty$ with such parameters of τ , it cannot exceed the value $\tau_m = 0.58 \sigma_m$. Let us consider the deformation compaction equation for the granulation process of bulk materials. To determine the stress state of a porous body, the first and the second terms of Equation (6) may be expressed as a function of τ and its derivative $\dot{\tau}_z$, using expressions (8) – (13):

$$\dot{\tau}_R = -0.58 \cdot \varepsilon^2 \cdot \sigma \cdot \dot{\sigma}_R \cdot (\sigma_m^2 - \varepsilon^2 \cdot \sigma^2)^{-0.5} = 0.33 \cdot \varepsilon \cdot \mu^{-1} \cdot \dot{\tau}_z \cdot \tau^{-1} \cdot (\sigma_m^2 - 3 \cdot \tau^2)^{0.5} \quad (17)$$

Equation (6) may be expressed as follows:

$$0.33 \cdot \varepsilon \cdot \tau^{-1} \cdot \mu^{-1} \cdot (\sigma_m^2 - 3 \cdot \tau^2)^{0.5} \cdot \frac{\partial \tau}{\partial z} - 3 \cdot \varepsilon^{-1} \cdot \tau \cdot (\sigma_m^2 - 3 \cdot \tau^2)^{-0.5} \cdot \frac{\partial \tau}{\partial z} + \frac{\tau}{R} = 0 \quad (18)$$

By performing the procedure of separation of variables and summing up the integration, the following is obtained:

$$0.6 \cdot \varepsilon \cdot \mu^{-1} \cdot \int \left(\frac{(0.3 \cdot \sigma_m^2 - \tau^2)^{0.5}}{\tau^2} \right) d\tau - 1.7 \cdot \varepsilon^{-1} \cdot \int (\sigma_m^2 - \tau^2)^{-0.5} d\tau + R_1^{-1} \cdot \int dz = 0 \quad (19)$$

$$0.33 \cdot \varepsilon \cdot \mu^{-1} \cdot \tau^{-1} \cdot (\sigma_m^2 - 3 \cdot \tau^2)^{0.5} + [0.58 \cdot \varepsilon \cdot \mu^{-1} + 1.73 \cdot \varepsilon^{-1}] \cdot \sin^{-1} [1.73 \cdot \tau \cdot \sigma_m^{-1}] - z \cdot R_1^{-1} = C \quad (20)$$

or considering (8):

$$\sigma \cdot \omega^{-1} \cdot \tau^{-1} + \chi \cdot \beta - z \cdot R_1^{-1} = C \quad (21)$$

where:

$$\chi = 0.58 \cdot \varepsilon \cdot \mu^{-1} + 1.73 \cdot \varepsilon^{-1}; \beta = \sin^{-1} [1.73 \cdot \tau \cdot \sigma_m^{-1}]; \omega = 3 \cdot \mu \cdot \varepsilon^{-2} \quad (22)$$

The integration constant C can be found by taking into account the initial and the limiting conditions. At the beginning of plastic deformation on the contact surface between the die and the roller during the granulation process, that is, at $z = h = H_0$ and $R = R_1$, the tangential stress reaches a value equal to the plasticity constant: $\tau = \eta = 0.58 \sigma_m$, and, taking into account condition (7), it is established that the normal stress becomes zero: $\sigma = 0$. Therefore:

$$C = 0.5 \cdot \chi \cdot \pi - H_0 \cdot R^{-1} \quad (23)$$

Then the solution (21) is expressed in the following way:

$$\sigma \cdot \omega^{-1} \cdot \tau^{-1} + \chi \cdot \beta - z \cdot R_1^{-1} = 0.5 \cdot \chi \cdot \pi - H_0 \cdot R^{-1} \quad (24)$$

By substituting $R = R(z)$ into expression (24), the marginal conditions can be satisfied. For a cylindrical die $R = \text{const}$, the value remains constant.

Equation (24) defines the equation of deformation compaction of a porous body, which connects all parameters of the process. To determine stresses σ and τ , this equation must be solved together with the plasticity condition (7), namely, by substituting expressions (8), (9):

$$(\sigma_m^2 - 3 \cdot \tau^2)^{0.5} \cdot \omega^{-1} \cdot \tau^{-1} \cdot \varepsilon^{-1} + \chi \cdot \beta - z \cdot R_1^{-1} = 0.5 \cdot \chi \cdot \pi - H_0 \cdot R^{-1} \quad (25)$$

$$1.73 \cdot (\sigma_m^2 - \varepsilon^2 \cdot \sigma^2)^{-0.5} \cdot \omega^{-1} \cdot \sigma + \chi \cdot \beta - z \cdot R_1^{-1} = 0.5 \cdot \chi \cdot \pi - H_0 \cdot R^{-1} \quad (26)$$

Equations (24)–(26) are transcendental, but functions $\sigma(z, R)$ and $\tau(z, R)$ are given implicitly. Their solution is possible only with the help of numerical methods. However, these equations are a closed solution for the problem of axisymmetric granulation theory of porous bodies under the condition of plasticity.

Let us represent the first term in equation (6) as function of σ and its derivative, using expressions (10), (12), (13):

$$\begin{aligned} \dot{\tau}_R &= -0.58 \cdot \varepsilon^2 \cdot \sigma \cdot \dot{\sigma}_R \cdot (\sigma_m^2 - \varepsilon^2 \cdot \sigma^2)^{-0.5} = \\ &= -0.58 \cdot \varepsilon^2 \cdot \sigma \cdot \dot{\tau}_z \cdot \mu^{-1} \cdot (\sigma_m^2 - \varepsilon^2 \cdot \sigma^2)^{-0.5} = \\ &= -0.33 \cdot \varepsilon^4 \cdot \sigma^2 \cdot \dot{\sigma}_z \cdot \mu^{-1} \cdot (\sigma_m^2 - \varepsilon^2 \cdot \sigma^2)^{-1}. \end{aligned} \quad (27)$$

Equation (6) can be rewritten as follows:

$$-0.33 \cdot \varepsilon^4 \cdot \sigma^2 \cdot \mu^{-1} \cdot (\sigma_m^2 - \varepsilon^2 \cdot \sigma^2)^{-1} \cdot \frac{\partial \sigma}{\partial z} + \frac{\partial \sigma}{\partial z} + \frac{\tau}{R} = 0 \quad (28)$$

Both parts of the equation are divided by τ , using the substitution of expression (9):

$$-0.33 \cdot \varepsilon^4 \cdot \sigma^2 \cdot \mu^{-1} \cdot \tau^{-1} \cdot (\sigma_m^2 - \varepsilon^2 \cdot \sigma^2)^{-1} \cdot \frac{\partial \sigma}{\partial z} + \tau^{-1} \cdot \frac{\partial \sigma}{\partial z} + R^{-1} = 0 \quad (29)$$

$$-0.58 \cdot \varepsilon \cdot \sigma^2 \cdot \mu^{-1} \cdot \left(\left[\frac{\sigma_m}{\varepsilon} \right]^2 - \sigma^2 \right)^{-1.5} \cdot \frac{\partial \sigma}{\partial z} + 1.73 \cdot \varepsilon^{-1} \cdot \left(\left[\frac{\sigma_m}{\varepsilon} \right]^2 - \sigma^2 \right)^{-0.5} \cdot \frac{\partial \sigma}{\partial z} + R^{-1} = 0 \quad (30)$$

By separating variables and integrating, it is obtained:

$$-0.58 \cdot \varepsilon \cdot \mu^{-1} \cdot \int \left[\sigma^2 \cdot \left(\left[\frac{\sigma_m}{\varepsilon} \right]^2 - \sigma^2 \right)^{-1.5} \right] d\sigma + 1.73 \cdot \varepsilon^{-1} \cdot \int \left(\left[\frac{\sigma_m}{\varepsilon} \right]^2 - \sigma^2 \right)^{-0.5} d\sigma + \int R^{-1} dz = 0 \quad (31)$$

$$-0.58 \cdot \varepsilon \cdot \mu^{-1} \cdot \left[\sigma \cdot \left(\left[\frac{\sigma_m}{\varepsilon} \right]^2 - \sigma^2 \right)^{-0.5} - \sin^{-1} \left[\varepsilon \cdot \sigma \cdot \sigma_m^{-1} \right] \right] + 1.73 \cdot \varepsilon^{-1} \cdot \sin^{-1} \left[\varepsilon \cdot \sigma \cdot \sigma_m^{-1} \right] + z \cdot R^{-1} = C \quad (32)$$

$$\left[0.58 \cdot \varepsilon \cdot \mu^{-1} + 1.73 \cdot \varepsilon^{-1} \right] \cdot \sin^{-1} \left[\varepsilon \cdot \sigma \cdot \sigma_m^{-1} \right] - 0.58 \cdot \varepsilon^2 \cdot \mu^{-1} \cdot \sigma \cdot (\sigma_m^2 - \varepsilon^2 \cdot \sigma^2)^{-0.5} + z \cdot R^{-1} = C \quad (33)$$

Or, taking into account (9) and (12):

$$\chi \cdot \alpha - \sigma \cdot \omega^{-1} \cdot \tau^{-1} + z \cdot R_1^{-1} = C \quad (34)$$

The constant of integration C can be determined using the initial and marginal conditions, for example, when $z = h = H_0$ and $R = R_1$. During the start of plastic deformation when $\tau = \eta = 0.58 \sigma_m$, $\sigma = 0$, the value of C will be equal to H_0 / R . The resulting solution (34) takes the following form:

$$\chi \cdot \alpha - \sigma \cdot \omega^{-1} \cdot \tau^{-1} + z \cdot R_1^{-1} = H_0 \cdot R^{-1} \quad (35)$$

Comparing Equations (24) and (35), it can be concluded that they essentially express the same equation, differing only in the angles α and β , as shown in (Fig. 3). By adding their left and right parts, the plasticity condition is obtained (7), which is expressed by the angles α and β :

$$\sin^{-1} \left[1.73 \cdot \tau \cdot \sigma_m^{-1} \right] + \sin^{-1} \left[\varepsilon \cdot \sigma \cdot \sigma_m^{-1} \right] = \alpha + \beta = \pi / 2 \quad (36)$$

Equation (35) can also be obtained from equation (24) by replacing β angle with angle $\alpha: \beta = \alpha - \pi / 2$.

The presence of trigonometric functions of angles in the equation of deformation compaction is a result of the relationship between normal and tangential stresses σ and τ according to the algebraic dependence (7).

To find stresses σ and τ using simple formulas, the specifics of axisymmetric loading are used. Let us turn again to Fig. 3. The nominal cross-section in the granulation channel, as well as the plasticity circle, have the shape of a circle with radius R . The point under consideration O_1 is located on a circle with radius R_1 . The section of this circle with diagonal OO_2 of triangle OO_2B_2 yields point O_1 that has the same coordinates z and R_1 , and is also in the same stress state as point O_1 . The projection of radius $R_1(OO_1)$ onto axis $\tau(R)$ forms segment $R_2(OB_1)$ and creates a coordinate triangle OO_1B_1 . Right triangles OO_2B_2 and OO_1B_1 with the same angles α and β have geometric similarities, that is:

$$\begin{aligned} \zeta = \sin \beta &= \frac{R_2}{R_1} = 1.73 \cdot \tau^{-1} \cdot \sigma_m^{-1} \\ \cos \beta &= \varepsilon \cdot \sigma \cdot \sigma_m^{-1} = \frac{\sqrt{R_1^2 - R_2^2}}{R_1} = \sqrt{1 - \left[\frac{R_2}{R_1} \right]^2} = \sqrt{1 - \zeta^2} \\ \sigma \cdot \tau^{-1} &= 1.73 \cdot \varepsilon^{-1} \cdot [\tan \beta]^{-1} \cdot 1.73 \cdot \varepsilon^{-1} \cdot \beta^{-1} \\ \sigma &= \sigma_m \cdot \varepsilon^{-1} \cdot \sqrt{1 - \zeta^2}; \quad \tau = 0.58 \cdot \zeta \cdot \sigma_m \end{aligned} \quad (37)$$

To calculate stresses σ and τ using formulas (37), it is sufficient to find the value of angle β and coefficient ζ . Let's substitute ratio σ/τ from formula (37) into (24), After minor transformations, a quadratic three-term equation is obtained, from which angle β is determined, and then coefficient ζ :

$$a \cdot \beta^2 + b \cdot \beta + c = 0; \beta_{1,2} = \frac{-b \pm \sqrt{b^2 - 4 \cdot a \cdot c}}{2 \cdot a}$$

where:

$$a = \chi \cdot \omega \cdot \varepsilon; b = -\eta \cdot \omega \cdot \varepsilon; c = 1.73; \eta = \chi \cdot \frac{\pi}{2} - \frac{H_0}{R} + \frac{z}{R_1}; \zeta = \sin\beta \quad (38)$$

The coefficient ζ is a complex function of the coordinates of the points within the elementary volume undergoing deformation, the relative density of the granules, and the yield strength of the material being deformed at a given temperature and granulation speed mode.

The system of equations (37), (38) is a closed analytical solution to the equation of deformation compaction of a porous body. In addition to calculations and analysis of local characteristics of the stress state of the granulation process, these equations allow determining the integral parameters of this process: of pressure, the force and deformation work.

The force calculation of the granulation process will be carried out by constructing force diagrams and determining the deformation work, which are related to the determination of the average integral value of pressure on the contact surface between the material and the die during the granulation process S at $z=h$, $R = R_1$. The average pressure, without taking into account the contact friction forces, is calculated using the following formula:

$$\begin{aligned} g_i &= \frac{1}{S_i} \cdot g_i(S) \cdot dS = \frac{1}{S_i} \cdot [\sigma_z + \tau_{zR}] \cdot dS = \frac{1}{\pi \cdot R_1^2} \int_0^R \left[\frac{\sigma_m}{\varepsilon} \cdot \sqrt{1-\zeta^2} + \frac{\zeta \cdot \sigma_m}{\sqrt{3}} \right] d(\pi \cdot R^2) = \\ &= \frac{2 \cdot \sigma_m}{R_1^2} \int_0^R \left[\frac{1}{\varepsilon} \cdot \sqrt{1-\zeta^2} + \frac{\zeta}{\sqrt{3}} \right] \cdot R \cdot dR. \end{aligned} \quad (39)$$

Based on the results of numerical integration (39), a diagram of the granulation process $g_i(\mu)$ is constructed, considering that $\varepsilon = 1-\mu$. It is important to note here that plastic deformation of the material does not occur at a zero value of the average pressure during the granulation process, calculated on the contact area. At the beginning of the process, the average pressure has a clearly defined value, which was taken into account when determining the initial and the marginal conditions and which can be calculated using formula (39).

The formula for the calculation of the force of the granulation process is as follows (Pisarenko & Mozharovsky, 1981; Bratishko, 2014; Bratishko, 2014):

$$P_i = g_i \cdot S_i = 2 \cdot \pi \cdot \sigma_m \cdot \int_0^R \left(\left[\varepsilon^{-1} \cdot \sqrt{1-\zeta^2} + \frac{\zeta}{\sqrt{3}} \right] \cdot R \right) dR \quad (40)$$

The impact of the contact friction forces is considered taking into account the efficiency of granulation processes of porous materials, which largely depends on the interaction of the lateral surface of granulation with the wall of the die, especially when the movement occurs. The speed of the movement of the material particles along the height of the spinneret during the granulation process decreases from the maximum value \mathcal{G} to zero, this means that the roller moves at a constant speed \mathcal{G} . This results in a lateral friction force that consistently counteracts the effective force exerted by the roller on the material during the granulation process. This interaction positively influences the process flow by reducing deformation resistance and lowering the energy required for deformation work.

The average value of the normal lateral pressure is calculated as (Zhou et al., 2021; Probst & Ileleji, 2016):

$$g_R = \frac{1}{h} \cdot \int_0^h [\sigma_R(z) + \tau_{Rz}(z)] dz = \sigma_m \cdot h^{-1} \cdot \int_0^h \left[\mu \cdot \varepsilon^{-1} \cdot \sqrt{1-\zeta^2} + \frac{\zeta}{\sqrt{3}} \right] dz \quad (41)$$

The Amonton-Coulomb law shows that the frictional force between the surfaces is proportional to the lateral pressure (Pisarenko & Mozharovsky, 1981; Bratishko, 2014; Bratishko, 2020):

$$\tau = f \cdot g_R = f \cdot \sigma_m \cdot h^{-1} \cdot \int_0^h \left[\mu \cdot \varepsilon^{-1} \cdot \sqrt{1 - \zeta^2} + \frac{\zeta}{\sqrt{3}} \right] dz \quad (42)$$

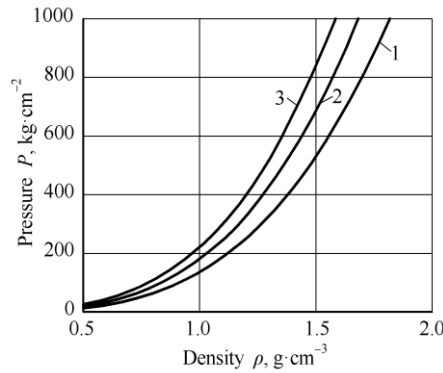


Fig. 4 – Dependence of specific pressing pressure P on the density of the material ρ for various values of the physical and mechanical properties of the material mixture

1 – $\delta = 141.4$; 2 – $\delta = 183.2$; 3 – $\delta = 220.6$

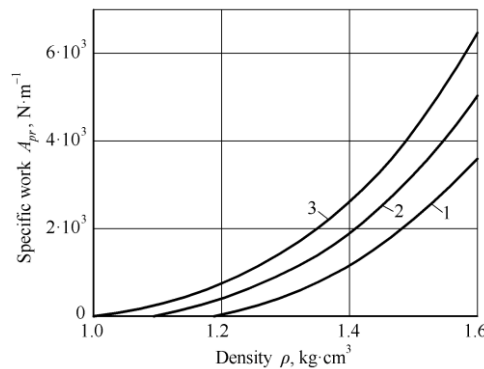


Fig. 5 – Dependence of the specific work A_{pr} of the granulation process on the density ρ of the material for various values of the physical and mechanical properties of the material mixture:

1 – $\delta = 141.4$; 2 – $\delta = 183.2$; 3 – $\delta = 220.6$

The lateral friction force is defined as the result of multiplying the specific friction force by the area of the lateral contact surface of the die during the granulation process. This ratio shows how the friction force depends upon the contact area and the magnitude of the specific friction force:

$$F_T = \tau \cdot S_R = 2 \cdot \pi \cdot R \cdot f \cdot \sigma_m \cdot \int_0^h \left[\mu \cdot \varepsilon^{-1} \cdot \sqrt{1 - \zeta^2} + \frac{\zeta}{\sqrt{3}} \right] dz \quad (43)$$

With this conclusion it can be claimed that the lateral friction force is determined by the contact area between the granulation surface and the bulk material that is supplied for granulation. This is of great importance in the analysis and calculation of the force parameters of the granulation process and the reduction of deformation resistance.

To take into account the impact of the contact friction forces during the granulation of a porous body in the moving die, the following calculation expression is used:

$$P = P_i - F_T = 2 \cdot \pi \cdot \sigma_m \cdot \left[\int_0^R \left(\left[\varepsilon^{-1} \cdot \sqrt{1 - \zeta^2} + \frac{\zeta}{\sqrt{3}} \right] \cdot R \right) dR - R \cdot f \cdot \int_0^h \left[\mu \cdot \varepsilon^{-1} \cdot \sqrt{1 - \zeta^2} + \frac{\zeta}{\sqrt{3}} \right] dz \right] \quad (44)$$

The displacement of deformation and the relative density of granules during the granulation process are related by the following relationship:

$$\Delta h = H_0 - H \cdot \mu^{-1} \quad (45)$$

Accordingly, the expressions for calculating the current value of the deformation work and the total work have the following form:

$$A_p = \int_0^{\Delta h} P(\Delta h) d(\Delta h) = \int_{\mu_0}^{\mu} P(\mu) d\mu \quad (46)$$

$$A_z = \int_0^{H_0-H} P(\Delta h) d(\Delta h) = \int_{\mu_0}^{\mu_k} P(\mu) d\mu \quad (47)$$

The above equations and formulas facilitate the calculations and analysis of the force parameters of the granulation process of porous bodies. They allow taking into account the impact of contact friction forces upon the process, which helps to determine the efficiency of the proposed process flow diagram and energy costs for deformation.

It should be noted that granulated materials have several advantages over the bulk materials. One of the main limiting factors for the widespread use of granulation is the low energy efficiency of the existing granulators. For example, the ring die granulators with a capacity of up to $1 \text{ t}\cdot\text{h}^{-1}$ are equipped with drive electric motors with a power of 90-110 kW.

Based on our calculations, innovative energy-efficient granulators are being developed from the original design of the press rollers and the annular die. A possibility to obtain granules from some types of both agricultural and wood processing raw materials has been experimentally proven. The research is carried out on a specially created experimental setup, which is shown in Fig. 6. Taking into account that the parameters of granulation processes influence a number of input factors, the granulation processes must be described by multifactorial dependencies that can be obtained on the basis of the theory of planning multifactorial experiments. To formulate the planning task correctly, it is necessary to conduct preliminary studies of the impact of individual factors.

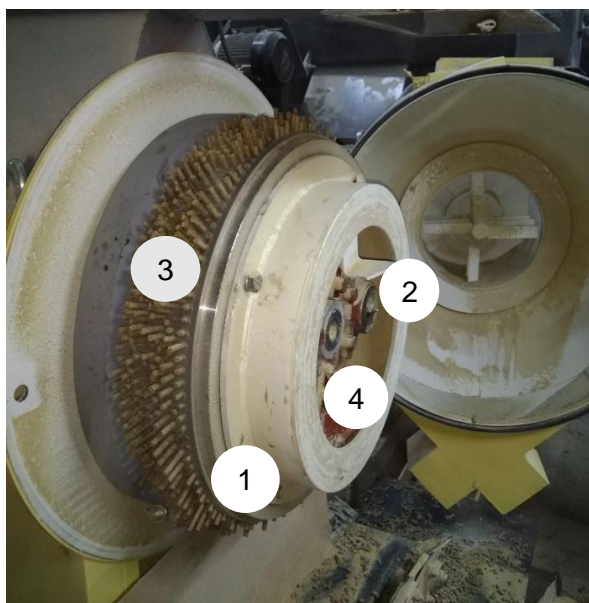


Fig. 6 – Experimental setup for granulating agricultural waste
1 – die; 2 – roller; 3 – granulate material; 4 – spinneret

During the experiments, the granulation system was used to process agricultural waste as well as wood-processing raw materials. The raw material was fed using a screw conveyor with adjustable drive shaft speed. The input parameters identified as influencing pellet quality and production efficiency were: temperature, raw material moisture content, the rotational speed of the gear transmission pinion, n , (rpm), and the screw shaft speed, n_w , (rpm). The raw material temperature was measured using a pyrometer-thermometer (model AZ-8838), and moisture content was measured with a Greisinger GMK100 non-contact moisture meter. The diameter of the die holes was 8 mm. Granulation productivity Q and pellet density ρ were selected as the main evaluation criteria. Productivity was determined using the well-known formula $Q = m \tau^{-1}$ ($\text{kg}\cdot\text{h}^{-1}$), where m is the mass of granules, obtained over time t .

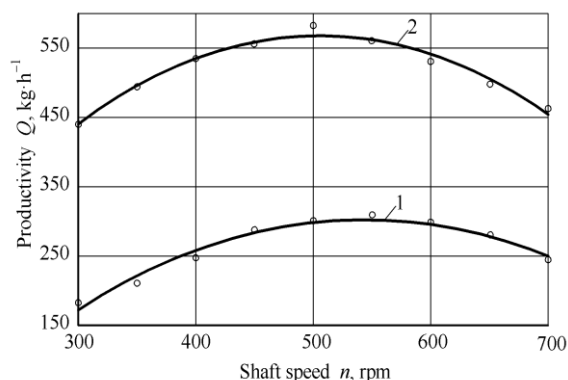


Fig. 7 – Dependence of granulation productivity of agricultural raw materials on the number of revolutions of granulator’s leading shaft ($d = 8 \text{ mm}$; $n_w = 20 \text{ rpm}$; $T = 14^\circ\text{C}$; $W = 34.8\%$)
 1 – two-roller granulation system; 2 – three-roller granulation system

Fig. 7 shows dependence of granulation productivity of agricultural raw materials on the number of drive shaft revolutions. It is evident that the dependencies have an optimum in the range of 500 – 550 rpm. In addition, it was found that when the material sticks to the die, the productivity decreases by 1.5-2.0 times. It is necessary to determine the factors that influence the nature of the free (without sticking) exit of granules through the holes of the die. During granulation of the raw materials its humidity and temperature were taken into account.

Fig. 8 presents the graphical dependence of the granulation productivity of woodworking raw materials on the number of revolutions of the granulator’s leading shaft.

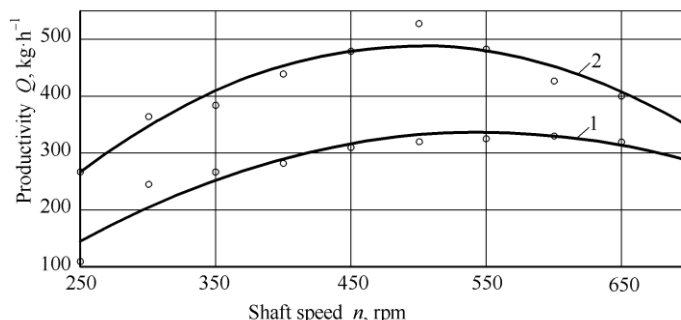


Fig. 8 – Dependence of granulation productivity of woodworking raw materials on the number of revolutions of the granulator’s leading shaft ($d = 8 \text{ mm}$; $n_w = 20 \text{ rpm}$; $T = 14^\circ\text{C}$; $W = 25.4\%$)
 1 – two-roller granulation system; 2 – three-roller granulation system

It has been established that dependence $Q(n)$ is also of an extreme nature. Maximum productivity (over $320 \text{ kg}\cdot\text{h}^{-1}$) is observed in the range of rotational speeds of the granulator’s leading shaft – from 600 to 700 rpm.

One of the key quality indicators of granules is their density, which was measured both immediately after production and after cooling. To determine granule density, samples with identical moisture content and temperature were taken, but produced at varying screw conveyor shaft speeds $n_w = 10 - 70 \text{ rpm}$, while maintaining a constant rotational speed of the granulator’s leading shaft $n = 500 \text{ rpm}$. The tests were conducted at different initial raw material moisture contents: 15.1%, 25.4%, and 34.8%.

The data, obtained during the experiment, are presented in Table 1.

Table 1

Density of granules of the agricultural raw materials depending on the number of revolutions of the screw conveyor "before cooling" / "after cooling" at different humidity of the raw materials

Number of screw revolutions n_w , rpm	Density of granules ρ , kg·m ⁻³ at various raw material moisture					
	15.1%		25.4%		34.8%	
	before cooling	after cooling	before cooling	after cooling	before cooling	after cooling
10	1252.2	1181	1140.3	1120.1	1011.2	951.8
20	1181.8	1123.4	1157.4	1120.9	1065.4	1023.2

Number of screw revolutions n_w , rpm	Density of granules ρ , kg·m ⁻³ at various raw material moisture					
	15.1%		25.4%		34.8%	
	before cooling	after cooling	before cooling	after cooling	before cooling	after cooling
30	1142.4	1078.9	1131.7	1102.6	1053.2	987.2
40	1210.2	1157.1	1110.2	1113.4	1034.4	974.5
50	1194.6	1078.5	1109.9	1100.5	1036.1	967.4
60	1248.3	1167.7	1134.4	1137.5	1011.5	996.6
70	1242	1185.9	1140.3	1120.4	1030.1	950.7

A graphical representation of the results of the experiment with a change in the granule density from the number of revolutions of the screw conveyor before and after cooling is shown in Fig. 9. It can be seen that the density remains almost constant, changing within 10%.

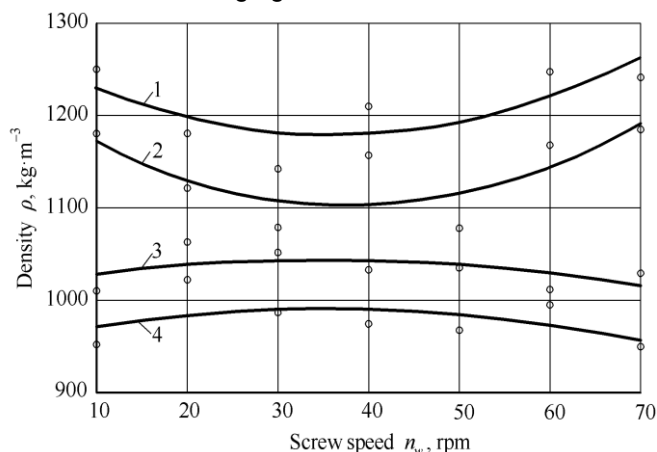


Fig. 9 – Graphic dependencies of the change of the granule density before and after cooling
 1 – granules before cooling; 2 – granules after cooling; ($d = 8$ mm; $T = 140^\circ\text{C}$; $W = 15.1\%$); 3 – granules before cooling;
 4 – granules after cooling; ($d = 8$ mm; $T = 140^\circ\text{C}$; $W = 34.8\%$)

The graphs presented in Fig. 9 show that the density of the granules, regardless of the initial moisture content of the raw material (from 15% to 35%), is practically independent of their cooling but depends on the feed rate of the raw material into the granulation zone. Thus, with an initial raw material moisture content of 34.8% an extreme value may be observed at the screw speed of $n_w = 20\text{--}30$ rpm (Fig. 9).

Under the condition of lower initial raw material moisture content (15.1%) the granules obtained have a denser structure ($\rho \approx 1200$ kg m⁻³), and with high initial raw material moisture content (more than 35%), the density of the obtained granules decreases to $\rho \approx 950$ kg·m⁻³. In addition, it should be said that in the operating mode of the granulator ($n = 500$ rpm and $n_w = 50$ rpm), in which the highest productivity is observed, the density of the granules is the lowest.

A series of preliminary experimental studies showed that the selected input factors have a significant impact on the initial parameters of the granulation process, which allows constructing correctly a plan for conducting multifactorial studies and identifying mathematical dependencies that describe the granulation process.

CONCLUSIONS

The application of the continuum model to the force calculation of the granulation process of porous bodies made it possible to obtain a comprehensive analytical solution for an axisymmetric problem. Application of the continuum model to the force calculation of the granulation process of porous bodies made it possible to obtain a complex analytical solution for an axisymmetric problem. The obtained mathematical dependencies take into account the differential equations of equilibrium and the plasticity condition. Since this solution applies to bodies of revolution of general shape and setting, it can be used for any axisymmetric loading scheme.

Equations for deformation compaction of a porous body have been obtained, both for an ideal granulation process and taking into account the forces of contact friction.

A method has been developed for calculation of local parameters of the stress state during the granulation process, using the coordinates of the plastic deformation point, as well as integral process parameters, such as pressure, force and the deformation work.

It was established that under the conditions of initial raw material moisture content (15.1%), the granules obtained have a denser structure ($\rho \approx 1200 \text{ kg m}^{-3}$), and with high initial raw material moisture content (more than 35%), the density of the obtained granules decreases to $\rho \approx 950 \text{ kg m}^{-3}$. In addition, it should be said that in the operating mode of the granulator ($n = 500 \text{ rpm}$ and $n_w = 50 \text{ rpm}$), in which the highest productivity is observed, the density of the granules is the lowest.

REFERENCES

- [1] Aruffo, G.A., Michrafy, A., Oulahna, D., Michrafy, M. (2024). Experimental and numerical analysis of structural inhomogeneity of grooved compacts. *Powder Technology*. Vol. 445. 120140.
- [2] Aruffo, G.A., Michrafy, M., Oulahna, D., Michrafy, A. (2022). Modelling powder compaction with consideration of a deep grooved punch. *Powder Technology*. Vol. 395, pp. 681-694
- [3] Benali M., Gerbaud V., Hemati M. (2009). Effect of operating conditions and physico-chemical properties on the wet granulation kinetics in high shear mixer. *Powder Technol.* 190(1):160–169.
- [4] Bertram, A. (2012). *Elasticity and Plasticity of Large Deformations*. Springer. 345 p.
- [5] Bettinotti, O., Allix, O., Perego, U., Oancea, V. & Malherbe, B. (2017). Simulation of delamination under impact using a global-local method in explicit dynamics. *Fin Elem Anal Des*. Vol.125, pp.1-13.
- [6] Boltyanska, N. (2018). Ways to Improve Structures Gear Pelleting Presses. TEKA. *An International Quarterly Journal on Motorization, Vehicle Operation, Energy Efficiency and Mechanical Engineering*. Lublin-Rzeszow. Vol.18, No 2, pp.23- 29.
- [7] Bratishko, V. (2014). Coordination of structural parameters of feed screw granulator matrices by pressure and throughput (Узгодження конструкційних параметрів матриць гвинтових грануляторів кормів за тиском та пропускною здатністю). *Technology in agricultural production, industry engineering, automation*. Issue 27. pp. 187-191. (in Ukrainian)
- [8] Bratishko, V. (2020). *Mechanical and technological bases for the preparation of complete feed using screw granulators*. Thesis Phd. Glewaha, 397. <https://doi.org/10.6084/m9.figshare.12370349.v1> (in Ukrainian)
- [9] Gurson, A.L. (1977). Continuum theory of ductile rupture by void nucleation and growth. *J. Eng. Mater. Techn.* № 2. pp.69-78.
- [10] Hashiguchi, K. & Yamakawa, Y. (2012). *Introduction to Finite Strain Theory for Continuum Elasto-Plasticity*. Wiley. 417 p.
- [11] Haupt, P. (2002). *Continuum Mechanics and Theory of Materials*. Springer. 643 p.
- [12] Landau, L.D., Lifshits, E.M. (2013). *Fluid Mechanics: Landau and Lifshitz: Course of Theoretical Physics*, Volume 6. 2nd edition, 538. Amsterdam: Pergamon.
- [13] Liu H., Wang K., Schlindwein W., Li M. (2013) Using the Box-Behnken experimental design to optimise operating parameters in pulsed spray fluidised bed granulation. *Int J. Pharm.* 448(2):329–338. doi: 10.1016/j.ijpharm.2013.03.057.
- [14] Lu, J., Li, L. (2017). Determining the reference geometry of plastically deformed material body undergone monotonic loading and moderately large deformation. *Fin. Elem. Anal. Des*. Vol.130, pp.1-11.
- [15] Lubliner, J. (1990). *Plasticity Theory*. Macmillan Publishing. 528 p.
- [16] Mangwandi C., Albadarin A.B., Ala'a H., Allen S.J., Walker G.M. (2013) Optimisation of high shear granulation of multicomponent fertiliser using response surface methodology. *Powder Technol.* 238:142–150.
- [17] Payne, J., Rattink, W., Smith, T. & Winowski, T. (2001). *Pelleting Handbook*. Sarpsborg, Borregaard Lignotech. 73 p.
- [18] Pietsch, W.B. (2002) *Agglomeration Processes. Phenomena, Technologies, Equipment*. Weinheim, Wiley-vch. 614 p.
- [19] Pisarenko, G. & Mozharovsky, N. (1981). *Equations and boundary value problems of the theory of plasticity and creep. Reference manual*. Naukova Dumka: Kiev. 496 p.
- [20] Probst, K.V., Ileleji, K.E. (2016). The effect of process variables on drum granulation behavior and granules of wet distillers grains with solubles. *Advanced Powder Technology*. Vol. 27, No. 4, pp.1347-1359

- [21] Salman, A.D., Hounslow, M.J. & Seville, J.P.K. (2007). *Handbook of Powder Technology. Granulation*. Vol. 11. Oxford. Elsevier, 1402 p.
- [22] Uniyal, S., Gandarillas, L.P., Michrafy, M., Oulahna, D., Michrafy, A. (2020). Analysis of densification mechanisms of dry granulated materials. *Advanced Powder Technology*. Vol. 31. pp.351-358.
- [23] Zheng, Y.N., Lu, H.F., Guo, X.L., Gong, X. (2017). Study on the effect of nanoparticles on the bulk and flow properties of granular systems. *Fuel Processing Technology*. Vol.177, pp. 30-38.
- [24] Zhou, H., Dahri, M.W., Zhou, M.X., Lai, Z.Y. (2021). Examining the effects of liquid-powder binder concentration on the cohesion and friction of a granular bed. *Particulate Science and Technology*. Vol. 39, No.7, pp.832-843.